Nuclear Materials and Energy 12 (2017) 234–240

Contents lists available at ScienceDirect

Nuclear Materials and Energy

journal homepage: www.elsevier.com/locate/nme

Main chamber wall plasma loads in JET-ITER-like wall at high radiated fraction

C. Guillemaut[a,b,*], P. Drewelow[c], G.F. Matthews[d], A.S. Kukushkin[e,f], R.A. Pitts[g], P. Abreu[b], S. Brezinsek[h], M. Brix[d], P. Carman[d], R. Coelho[b], S. Devaux[i], J. Flanagan[d], C. Giroud[d], D. Harting[d], C.G. Lowry[j], C.F. Maggi[d], F. Militello[d], C. Perez Von Thun[h], E.R. Solano[k], A. Widdowson[d], S. Wiesen[h], M. Wischmeier[l], D. Wood[d], JET Contributors[1]

[a] EUROfusion Consortium, JET, Culham Science Centre, Abingdon OX14 3DB, UK
[b] Instituto de Plasmas e Fusao Nuclear, Instituto Superior Tecnico, Universidade Lisboa, Lisboa, Portugal
[c] Max-Planck-Institut fur Plasmaphysik, Teilinstitut Greifswald, D-17491 Greifswald, Germany
[d] CCFE, Culham Science Centre, Abingdon OX14 3DB, UK
[e] NRC Kurshatov Institute, Akademika Kurchatova pl., 123182 Moscow, Russia
[f] NRNU MEPhI, Kashirskoje sh. 31, 115406 Moscow, Russia
[g] ITER Organization, Route de Vinon CS 90 046, 13067 Saint-Paul-Lez-Durance, France
[h] Forschungszentrum Jülich GmbH, Institut für Energie- und Klimaforschung—Plasmaphysik, 52425 Jülich, Germany
[i] Institut Jean Lamour, UMR7198 CNRS—Université de Lorraine, F-54506 Vandoeuvre-les-Nancy Cedex, France
[j] European Commission, B-1049 Brussels, Belgium
[k] Laboratorio Nacional de Fusión, CIEMAT, 28040 Madrid, Spain
[l] Max-Planck-Institut fur Plasmaphysik, 85748 Garching bei Munchen, Germany

ARTICLE INFO

Article history:
Received 13 July 2016
Revised 17 January 2017
Accepted 7 February 2017
Available online 10 March 2017

ABSTRACT

Future tokamak reactors of conventional design will require high levels of exhaust power dissipation (more than 90% of the input power) if power densities at the divertor targets are to remain compatible with active cooling. Impurity seeded H-mode discharges in JET-ITER-like Wall (ILW) have reached a maximum radiative fraction (F_{rad}) of ~75%. Divertor Langmuir probe (LP) measurements in these discharges indicate, however, that less than ~3% of the thermal plasma power reaches the targets, suggesting a missing channel for power loss. This paper presents experimental evidence from limiter LP for enhanced cross-field particle fluxes on the main chamber walls at high F_{rad}. In H-mode nitrogen-seeded discharges with F_{rad} increasing from ~30% to up to ~75%, the main chamber wall particle fluence rises by a factor ~3 while the divertor plasma fluence drops by one order of magnitude. Contribution of main chamber wall particle losses to detachment, as suggested by EDGE2D-EIRENE modeling, is not sufficient to explain the magnitude of the observed divertor fluence reduction. An intermediate detached case obtained at F_{rad} ~ 60% with neon seeding is also presented. Heat loads were measured using the main chamber wall thermocouples. Comparison between thermocouple and bolometry measurements shows that the fraction of the input power transported to the main chamber wall remains below ~5%, whatever the divertor detachment state is. Main chamber sputtering of beryllium by deuterium is reduced in detached conditions only on the low field side. If the fraction of power exhaust dissipated to the main chamber wall by cross-field transport in future reactors is similar to the JET-ILW levels, wall plasma power loading should not be an issue. However, other contributions such as charge exchange may be a problem.

1. Introduction

Future tokamak reactors of conventional design will have to dissipate more than 90% of the exhaust power to keep the heat flux densities at the divertor targets at levels acceptable for active cooling [1]. The JET-ITER-like Wall (ILW) [2] comprises a tungsten (W)

* Corresponding author at: Instituto de Plasmas e Fusao Nuclear, Instituto Superior Tecnico, Universidade Lisboa, Lisboa, Portugal.
E-mail addresses: christophe.guillemaut@ukaea.uk, cguillemaut@ipfn.ist.utl.pt (C. Guillemaut).

[1] See the Appendix of F. Romanelli et al., Proceedings of the 25th IAEA Fusion Energy Conference 2014, Saint Petersburg, Russia

http://dx.doi.org/10.1016/j.nme.2017.02.010

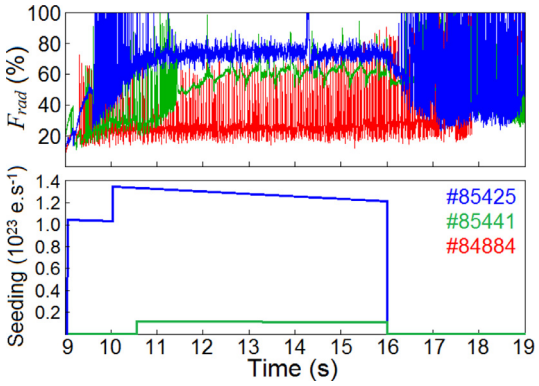

Fig. 1. Time traces of F_{rad} (top) and Ne and N seeding rates (bottom) in JET-ILW discharges.

Table 1
Distribution of exhaust power depending on divertor conditions.

	Unseeded	Ne seeded	N seeded
F_{rad}	30%	60%	75%
F_{div}	49%	13%	3%
Missing fraction	21%	27%	22%

divertor and beryllium (Be) main chamber wall thus matching the material configuration planned for ITER. Since W and Be are very poor radiators in the scrape-off layer (SOL), the seeding of impurities like nitrogen (N), neon (Ne) or argon (Ar) can be used to dissipate significant amounts of power radiatively. High power, N and Ne seeded H-mode discharges in JET-ILW have reached a maximum radiative fraction (F_{rad}) of ~75% and ~60%, respectively [3], see Fig. 1. However, the fraction of thermal plasma power reaching the targets (see Table 1) evaluated by surface integration of the power density profiles (Fig. 2) from divertor Langmuir probe (LP) measurements (see the positions in Fig. 3) is insufficient, suggesting a missing channel for the power loss.

As suggested by 2D fluid-neutral modeling with EDGE2D-EIRENE [4–6], divertor detachment is caused by a combination of three particle loss channels: volume recombination, molecular activated recombination and cross-field transport [7]. Therefore some exhaust power may be dissipated on the main chamber wall by filamentary cross-field transport. The purpose of this paper is to study the relation between the main chamber wall plasma loads and divertor detachment. The deeply detached, maximum F_{rad} JET-ILW discharge #85,425 with N seeding offers good conditions for such study. Discharge #85,441 using Ne seeding provides intermediate detached conditions and #84,884 is the reference unseeded attached discharge. This series of experiments in JET-ILW used a low triangularity with inner and outer vertical target divertor configuration. The plasmas were sustained in a toroidal magnetic field of 2.6 T with a plasma current of 2.5 MA. During impurity seeding, the heating power was around ~18 MW and was provided by neutral beam injection (NBI) only.

Detachment can also be obtained with deuterium (D) radiation alone in H-mode [8] but requires a very high level of fueling given that D is not a very good radiator like N or Ne. Since strong fueling rates tend to trigger H-L transitions and density limit disruptions, such detachment scenario is unlikely to be relevant for a reactor which is why this case has not been studied here. However, detachment in H-mode with pure D occurs similarly as with N or Ne seeding and is expected to generate the same effects on the main chamber wall.

As shown in Fig. 3, two of the JET-ILW inner and outer wall guard limiters are equipped with poloidal arrays of respectively 16 and 20 LP which can be used to estimate the wall ion flux, even during diverted discharges when the plasma-wall distances are large. Particle flux densities (J_{sat}) on individual limiter LP during diverted operation are too small and noisy and voltage sweeps are too slow (~25 ms) to allow T_e measurements using a fit method on the current–voltage (I–V) characteristics. Therefore, the heat loads have been obtained using the main chamber wall thermocouples placed in the same limiters as the LP. Although wide angle infrared thermography is available for the main chamber wall, it could not be used for this purpose here because the level of the signal is too low and cannot be distinguished from the background noise. The ratio of the heat load to the particle flux density allows estimation of the ion impact energies and Be sputtering by D on the main chamber wall.

In this paper, the evolution of limiter LP particle fluence measurements with detachment is presented in Section 2. In Section 3, correlation of the limiter particle flux variations with changes in the edge density profiles and filament activity is discussed. In Section 4, the plasma heat loads on the main chamber wall are estimated by comparing the thermocouple with the bolometry measurements. Finally, Be sputtering by D on the main chamber wall is discussed in Section 5.

2. Particle fluence on main chamber wall limiters during radiative scenarios

Particle fluence has been calculated by time integration of LP J_{sat} measurements on inner and outer limiters over the ~10 s NBI flat top in the discharges #85,425, #85,441 and #84,884. Thus, particle fluence values in Fig. 4 are expected to have a negligible statistical error. Only the systematic error due to uncertainties on the probe area of collection because of sheath and finite Larmor radius effects may not be negligible but at the same time very difficult to estimate. However, these effects exist in all three discharges studied here thus the relative error is expected to be negligible. Therefore, comparisons between wall conditions in the three cases are considered possible without having to estimate the systematic error.

All J_{sat} measurements here have been obtained at a LP bias of −190 V and below where saturation of the ion current is assumed. For clarity and because of the strength of the signals, the poloidal profiles shown in Fig. 4 have been obtained from the LP closest to the center of the limiters and on the side exposed to the plasma (red dots in orange area in Fig. 3c and d). These values have been plotted against the s coordinate following the main chamber poloidal contour in anti-clockwise direction, starting from 0 at the edge of the inner divertor and ending at the lower edge of the inner limiter at around 10 m, see Fig. 3b. Since most of the inner limiter LP were not working in #84,884, this data has been completed with measurements made in the equivalent unseeded attached discharge #83,487.

In Fig. 4, the particle fluence on the outer limiter increases from the range ~1.8–2.8 × 10^{22} m^{-2} in attached conditions to ~5–7.5 × 10^{22} m^{-2} with Ne seeding and up to ~8–12 × 10^{22} m^{-2} with deeply detached N seeded divertor. On the inner limiter, the increase of the particle fluence goes from the range ~2.3–3 × 10^{22} m^{-2} in attached conditions to ~6–8 × 10^{22} m^{-2} with Ne seeding and with N seeding. In these discharges, the separatrix-wall distance ranges from 6 to 14 cm outboard and from 15 to 18 cm inboard.

The total amount of particles collected on the limiters during the NBI flat top is calculated by multiplying the fluence from each LP by their associated limiter area (see magenta zones in Fig. 3c and d) and summing the results. The counts for the different regions of the plasma chamber shown in Table 2 are obtained considering that there are 11 equivalent outer limiters and 10 inner

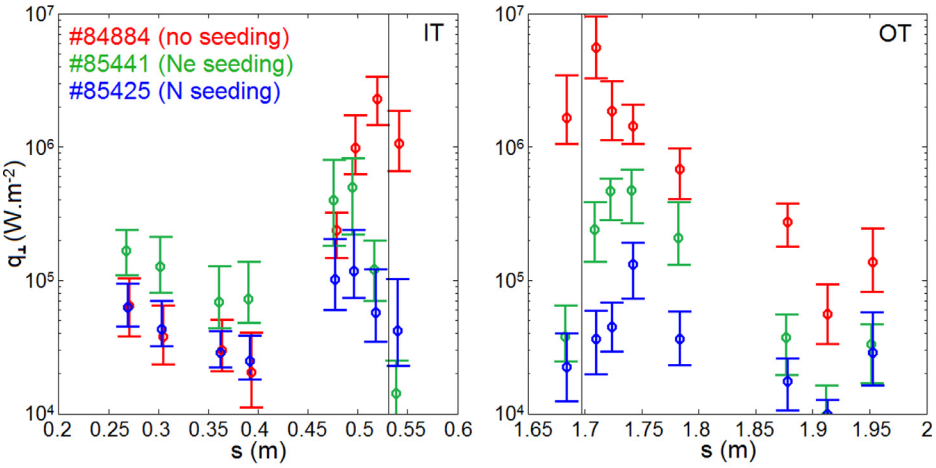

Fig. 2. Power density profiles on the inner (left) and outer (right) divertor target surfaces in JET-ILW discharges.

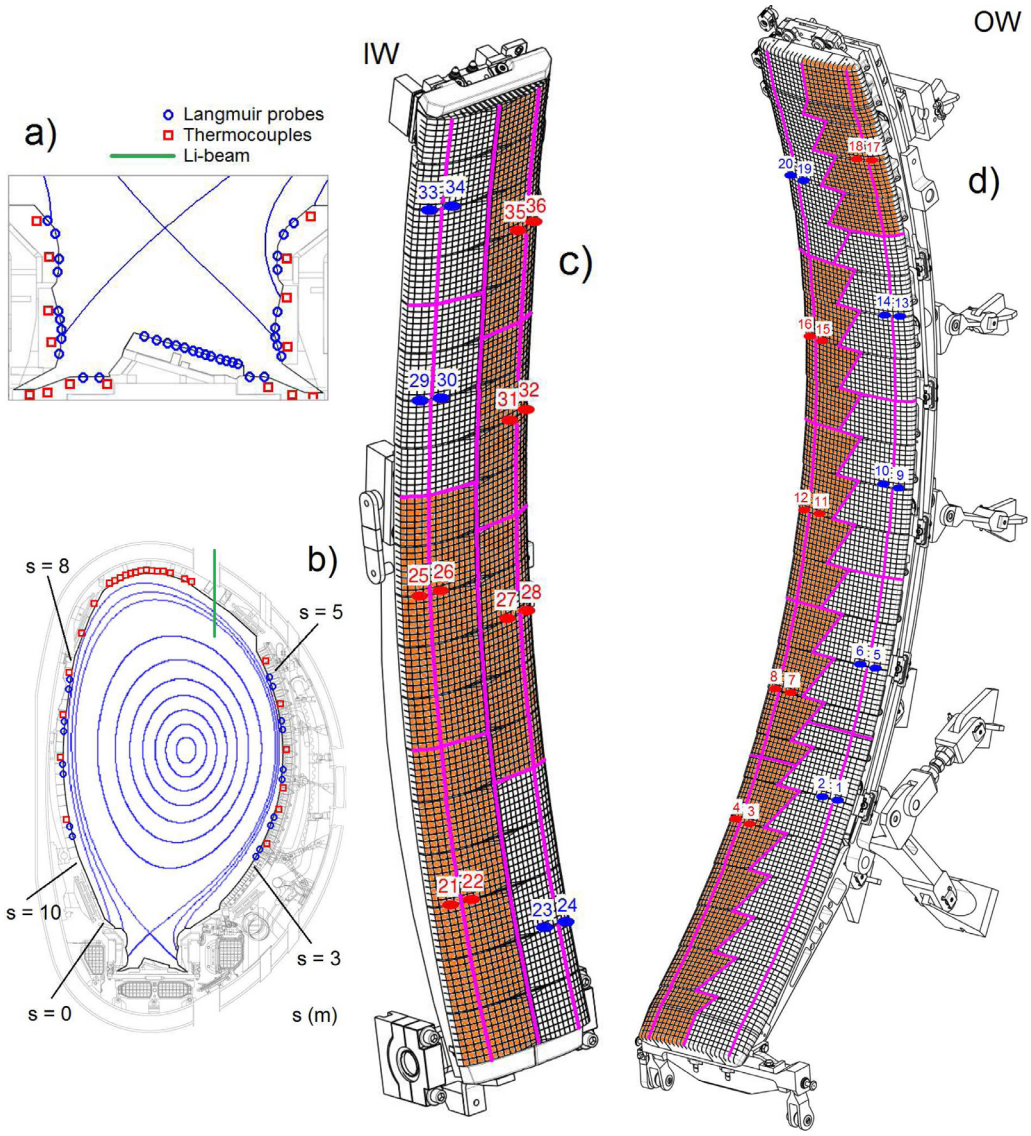

Fig. 3. (a) Position of divertor LP and thermocouples in the divertor. (b) The same for the main chamber. (c) Exposed (red dots in orange regions) and shadowed (blue dots) LP with their associated area of integration (magenta) on the inner guard wall limiter. (d) The same on the outer guard wall limiter. (For interpretation of the references to color in this figure legend, the reader is referred to the web version of this article.).

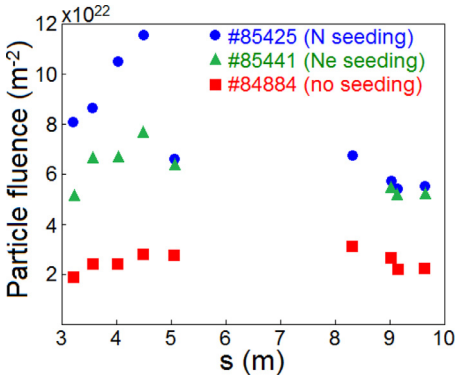

Fig. 4. Poloidal profiles of the particle fluence.

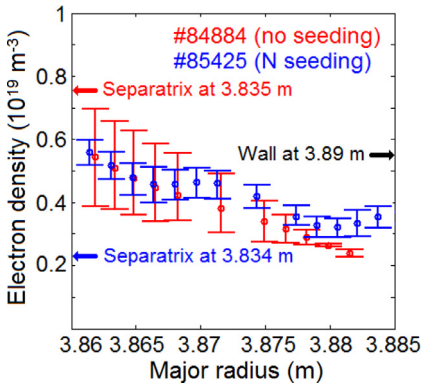

Fig. 5. Mid-plane electron density profile from Li-beam measurements.

Table 2
Distribution of total number of exhaust particles depending on divertor conditions.

	Unseeded	Ne seeded	N seeded
Outer wall	1.77×10^{23}	4.1×10^{23}	5.5×10^{23}
Inner wall	0.85×10^{23}	2×10^{23}	1.8×10^{23}
Divertor	61×10^{23}	27×10^{23}	6.6×10^{23}

limiters. In Ne seeded detached conditions, the total number of particles collected on the main chamber wall is increased by a factor ~2 compared to attached conditions while it is reduced by ~2 in the divertor. In N seeded detached conditions, the wall particle count increases by a factor ~3 compared to the attached case while it is reduced by a factor ~10 in the divertor. Overall, ~4% of the particles are transported to the main chamber wall limiters in attached conditions, ~18% in Ne detached conditions and ~52% in N detached conditions. It is worth mentioning that in all three cases, in Table 2, the particle count is at least ~2 times higher on the outer wall than on the inner wall. This is consistent with stronger filamentary transport due to unstable curvature driven mode on the low field side.

The idea that particle losses by cross-field transport contribute to some extent to divertor detachment is suggested by EDGE2D-EIRENE modeling [7,9]. However, between unseeded attached conditions and fully detached N seeded conditions, the divertor loses 54.4×10^{23} particles while the wall only gains 4.7×10^{23} particles, which indicates that the particle losses on the main chamber wall due to cross-field transport remain a minor contribution to the detachment process.

As discussed in [7,10], significant volume effects such as volume recombination and molecular activated recombination are likely to be involved to explain the enormous particle loss in the detached divertor of discharge #85,425. Recent work on JET-ILW using spectroscopy measurements to estimate the target electron density provides significantly higher values than LP [11]. Consequently, this suggests that T_e obtained from the latter is likely to be overestimated and therefore that the target plasma may be cold enough to allow significant particle losses through recombination processes.

3. Correlation of limiter particle flux with edge density profiles and filaments

In previous L-mode studies, enhanced particle loads on the main chamber wall in detached conditions were associated with broadening of the electron density (n_e) profile and enhanced filamentary cross-field transport, see [12–15]. In the experiments studied here, the far SOL mid-plane density was accessible through Li-Beam measurements (see Fig. 3) only in the unseeded attached case and the N seeded detached case. It is clear in Fig. 5 that n_e at 3.885 m is a factor ~1.5 higher when the divertor is detached.

A particular feature of high F_{rad} experiments is the disappearance of the Type I ELMs when $F_{rad} > 60$–65% with Ne and N seeding while the energy confinement time remains around ~300 ms as in unseeded attached conditions. Consistently with the previous Section results, comparison of J_{sat} measurements from limiter LP 11 (see Fig. 3d for the position) and the divertor LP shows opposite behaviors with an increase of the particle flux on the main chamber wall (Fig. 6a) while the divertor particle flux is strongly reduced during detachment (Fig. 6b and c). Inspection of high time resolution limiter LP 11 J_{sat} measurements reveals some particle bursts (Fig. 6a) which are only present in Ne and N seeded detached conditions when Type I ELMs have vanished. These structures can be observed on all limiter LP and are attributed to enhanced filamentary cross-field transport. They have a frequency of the order of ~1 kHz, which may be related to Type III ELMs activity. Unfortunately, due to the vertical target configuration, no diagnostics were available to confirm the presence of similar bursts matching this frequency in the divertor. The divertor LP voltage sweep was too fast to allow enough time during ion saturation to identify Type-III ELMs properly.

The transport of particles to the main chamber wall generates a plasma heat load that adds up to the radiative heat load. Both contributions are estimated in the next Section.

4. Plasma heat loads on main chamber wall during radiative scenarios

Limiter probe J_{sat} signals are too low and noisy and voltage sweeps are too slow (~25 ms) to allow T_e measurements using a fit method on the *I–V* characteristics. Coherent averaging over several sweeps of a signal cumulating ELM, inter-ELM filaments and possible other perturbations would not be of help either since steady conditions are required to obtain a meaningful T_e measurement with an *I–V* characteristic fit.

Therefore, heat loads have been obtained using the thermocouples embedded in some of the tiles of the main chamber wall, see Fig. 3b. They measure bulk tile temperatures in degree Celsius. Therefore, the energy Q_{tile} (in J) accumulated in a given tile during a discharge can be calculated with the temperature variation ΔT (in Celsius or K) between the beginning and the end of the discharge, the heat capacity C_p (in J kg^{-1} K^{-1}) of the tile material and its mass m (in kg) as follows:

$$Q_{tile} = mC_p\Delta T. \quad (1)$$

The main chamber tiles considered here are made of bulk Be with $C_p \sim 2390$ J Kg^{-1} K^{-1} in the range 100–200 °C of wall temperatures of JET-ILW. Q_{tile} given by the thermocouples accumulates

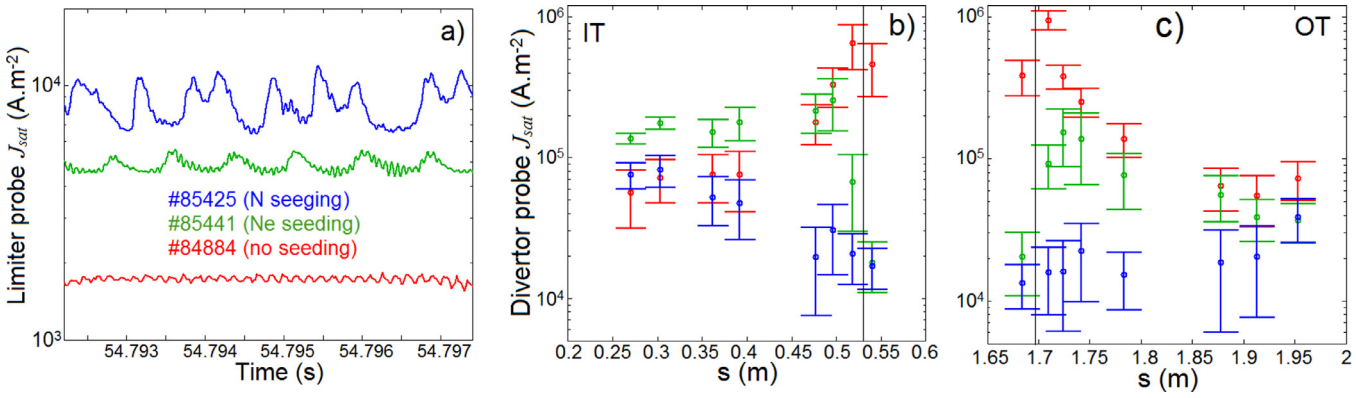

Fig. 6. (a) J_{sat} time trace from the limiter LP 11. (b) J_{sat} profile on the inner divertor target. (c) The same on the outer target.

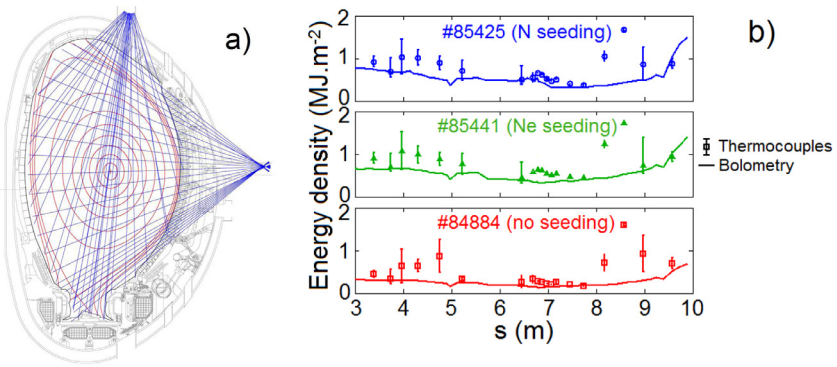

Fig. 7. (a) Bolometry lines of sight and (b) poloidal profiles of radiative and total energy density along the main chamber wall limiters.

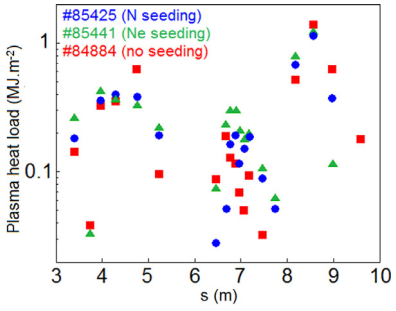

Fig. 8. Plasma contribution to poloidal profile of the energy density along the main chamber wall limiters.

the radiative, the plasma and possibly the charge exchange (CX) heating contributions.

The energy density in J m^{-2} can also be obtained by dividing Q_{tile} from (1) by the area of the tile surface exposed to the plasma flux and radiation. Energy density poloidal profiles from thermocouples are convenient to compare with the radiative energy densities deduced from bolometric tomographic reconstructions (Fig. 7a) to estimate the thermal power transported to the main chamber wall. According to [16], only the radiative contribution should fall in between limiters. Thus, the poloidal profile of radiative energy density on the main chamber wall, Fig. 7b, is axisymmetric while the profile of total energy density from the thermocouples exists only on limiters.

When the radiative contribution is subtracted from the total energy density profile on the limiters and if the CX is considered negligible on the limiters, the plasma contribution is obtained in Fig. 8, for the three cases considered here. Surface integration of the Fig. 8 profiles gives ~9 MJ, ~8.5 MJ and 8 MJ in unseeded, Ne seeded and N seeded conditions respectively. Since the limiter phase contribution to the wall heat load is of the order of ~2 MJ, not more than ~7 MJ are transported by the plasma to the main chamber wall during the diverted phase. The total input energy during the NBI flat top is around ~180 MJ in these experiments, thus only ~4% of it reaches the main chamber wall with the plasma, independently of the divertor detachment state. The peak power density is reached at the inner and outer mid-planes and does not exceed ~0.1 MW m^{-2} over the ~10 s NBI flat top. If this contribution remains at about the same fraction in a reactor, then the power loading by the radial plasma transport should not be an issue for the main chamber wall.

However, since this effect seems to be a minor contribution to the overall ~25% missing power loss (see Table 1) it is possible that another process like CX is involved, as discussed in [16]. Most of the neutrals responsible for CX are produced in the divertor and a few m away from its entrance this loss should be poloidally uniform on the main chamber wall where the limiters do not account for more than ~5% of the area in total. Therefore, most of the main chamber wall CX power should remain undetected in JET since it is expected to essentially fall in-between limiters or near the divertor entrance where thermocouples are absent. Even if such contribution exists on the part of the main chamber equipped with thermocouples, plasma heat flux due to cross-field transport would remain at least 5 times stronger than CX power on exposed limiter surfaces (Fig. 3c and d) in JET. Thus, the heat load estimates shown in Fig. 8 for the main chamber wall limiters are dominantly due to plasma power in any cases. As also discussed in [16], there is the possibility that the input power in JET is simply overestimated and in that case, a strong CX power loss channel does not need to be involved.

Mention has to be made that in a fusion reactor, a contribution from CX of the order of ~20% of the input power on the main

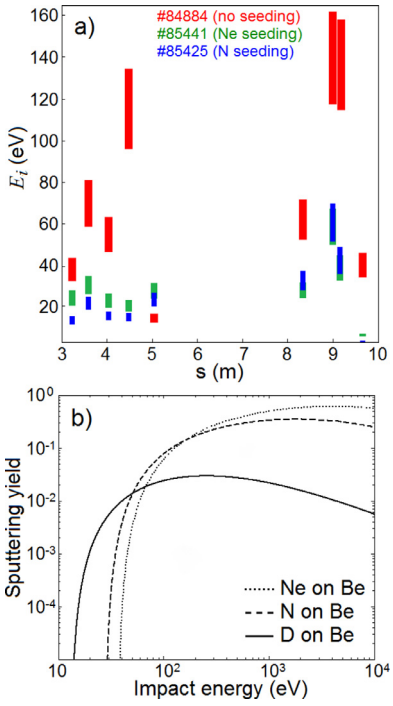

Fig. 9. (a) poloidal profiles of E_i along the inner and outer guard wall limiters and (b) Be sputtering yields from [16].

chamber wall would be an issue if it is not evenly distributed. Indeed, the impossibility of using copper in actively cooled components under heavy neutron irradiation and the lack of space in the first wall due to the presence of tritium breeding blanket modules should limit the maximum power density at a rather low value (~1 MW m^{-2}) according to [17,18].

5. Changes in main chamber wall sputtering with divertor detachment

On a given limiter tile surface of area A_{tile} exposed to the plasma, the particle fluence J is linked to Q_{tile} as follows:

$$\frac{Q_{tile}}{Q_{tile}} = (\gamma_i T_i + \gamma_e T_e) J, \tag{2}$$

with the ion and electron heat transmission coefficient $\gamma_i \sim 3.5$ and $\gamma_e \sim 5.5$ respectively [19] and the electron and ion temperature T_e and T_i (in eV) respectively. The ion impact energy E_i (in eV) on the limiters is defined as follows:

$$E_i = \gamma_i T_i. \tag{3}$$

If the SOL plasma is very collisional, $T_e \sim T_i$ and E_i becomes:

$$E_i = \left(\frac{\gamma_i}{\gamma_i + \gamma_e}\right)\frac{Q_{tile}}{JA_{tile}} \sim 0.39\frac{Q_{tile}}{JA_{tile}}. \tag{4}$$

As shown in [20,21], T_i can be up to $2T_e$ in JET SOL and in this case E_i is written as follows:

$$E_i = \left(\frac{2\gamma_i}{2\gamma_i + \gamma_e}\right)\frac{Q_{tile}}{JA_{tile}} \sim 0.56\frac{Q_{tile}}{JA_{tile}}. \tag{5}$$

Therefore, it is possible to use J and Q_{tile} measurements where limiter probes and thermocouples are physically close enough to deduce a range of E_i. The main chamber wall E_i poloidal profile in Fig. 9a is obtained by using the LP on the exposed side (in red in Fig. 3) closest to the limiter tile center and the associated thermocouples.

Table 3
Distribution of total number of sputtered Be atoms by D ions depending on divertor conditions.

	Unseeded	Ne seeded	N seeded
Outer wall	$2.2–2.6 \times 10^{21}$	$1–1.2 \times 10^{21}$	$2.1–2.5 \times 10^{20}$
Inner wall	$1.7–2 \times 10^{21}$	$1.1–1.3 \times 10^{21}$	$1.1–1.3 \times 10^{21}$

On the outer limiter, the E_i range goes up to ~130 eV at the mid-plane in unseeded conditions and falls down to an average of ~30 eV and then ~20 eV with Ne and N seeding respectively. On the inner limiter E_i can reach nearly ~160 eV at the mid-plane in attached conditions and drops to the range ~30–70 eV when detachment is obtained with Ne or N. These calculated E_i combined with the Be sputtering yields from [22] plotted in Fig. 9b allow an estimate of the main chamber limiter Be source in the discharges studied here. Be is dominantly sputtered by D and the source for the 11 outer and 10 inner guard wall limiters in total number of sputtered Be atoms is given in Table 3 for the three different divertor conditions. While no direct measurements of the impurity concentrations in the SOL were made, EDGE2D-EIRENE simulations predict that Ne and N concentrations of the order of a few percent are sufficient for strong radiative dissipation of exhaust power similarly as with carbon impurities in [7]. According to [23] the concentration of Be impurities should be of the order of ~1% in such discharges. This renders the contribution of the main impurities to Be sputtering an order of magnitude below that of D, given that the average energy of D ion hitting the wall is well above the sputtering threshold for Be, Fig. 9.

It is clear from Table 3 that detachment strongly reduces Be sputtering on the outer limiters while the effect is rather small on the inner limiters because of the weaker E_i reduction along with the increase of the particle flux. This is consistent with Be deposition observed on the upper inner divertor tiles in JET-ILW [24–27] and the stronger Be erosion observed on the inner limiters [28]. In the discharges studied here, the mass of Be sputtered by D from the inner limiters during the NBI flat top is of the order of ~25–30 mg in unseeded attached conditions and ~15–20 mg with N or Ne seeded detachment. These estimates do not account for a possible contribution from CX. According to [24], ~40 g of Be in total have been accumulated on the upper inner divertor tiles over the ~3000 discharges of the first JET-ILW campaign which represents an average of ~13 mg per discharge. Although this initial campaign mixed many different plasma configurations and input powers, it appears that Be sputtered from the inner limiters by direct plasma-wall interaction during the divertor phases may contribute significantly to the deposition observed on the inner divertor tiles. Thorough examination of the Be sputtering source from the guard wall limiters with the present method compared to spectroscopy measurements and post-mortem tile analysis should be the object of further studies.

6. Conclusions

Future tokamak reactors of conventional design will have to dissipate more than 90% of the exhaust power to keep heat flux densities at manageable levels on divertor targets [1]. Some exhaust power may be dissipated on the main chamber wall by cross-field filamentary transport, which could be an issue in the context of a reactor. Strongly detached high F_{rad} H-mode JET-ILW discharges have been used to study the relation between main chamber wall plasma loads and divertor detachment.

Particle fluence on the main chamber wall measured by limiter LP increases significantly with the level of divertor detachment. However, the amount of particles redirected to the main chamber wall corresponds to less than 10% of the amount miss-

ing in the fully detached divertor. Therefore, other stronger particle sinks must be involved to explain the magnitude of the particle fluence reduction observed by divertor LP during detachment. As suggested by EDGE2D-EIRENE modelling [7], spectroscopy measurements [11] and theoretical considerations [29], recombination processes may be the dominant contributors.

Main chamber power loads associated with cross-field transport have been estimated by thermocouples and bolometry measurements and make not more than 5% of the input power. If this fraction is similar in future reactors, the power loading by the plasma particles should not be an issue for the main chamber wall. However, since this effect seems to be a minor contribution to the overall ∼25% missing power loss (see Table 1), it is possible that another process like charge exchange is involved, as discussed in [16]. Such contribution of the order of ∼20% of the input power on the main chamber wall would be an issue for a fusion reactor if it is not evenly distributed given the strong power load limitations of the actively cooled first wall plasma facing components.

Particle fluence and power load measurements have been used to calculate the ion impact energy on the inner and outer guard wall limiters and estimate the Be sputtering source depending on the level of divertor detachment. Because of the small concentration of N, Ne or Be and the energy of impinging D ions well above the sputtering threshold, Be is dominantly sputtered by D on the limiters. It appears that detachment with impurity seeding strongly reduces the sputtering on the outer limiters but not on the inner limiters. This is consistent with Be deposition observed on the upper inner divertor tiles in JET-ILW [24–27] and the stronger Be erosion observed on the inner limiters [28]. This topic should be the object of further studies.

Acknowledgments

This work has been carried out within the framework of the EUROfusion Consortium and has received funding from the Euratom research. IST activities also received financial support from "Fundação para a Ciência e Tecnologia" through project UID/FIS/50010/2013. The views and opinions expressed herein do not necessarily reflect those of the ITER Organization or of the European Commission.

References

[1] G. Federici, et al., Fusion Eng. Des. 89 (2014) 882–889.
[2] G.F. Matthews, et al., Phys. Scr. T145 (2011) 014001.
[3] M. Wischmeier, J. Nucl. Mater. 463 (2015) 22–29.
[4] R. Simonini, et al., Contrib. Plasma Phys. 34 (1994) 368.
[5] D. Reiter, et al., J. Nucl. Mater. 196-198 (1992) 80.
[6] S. Wiesen, et al., 2006. ITC Project Report, http://www.eirene.de/e2deir_report_30jun06.pdf.
[7] C. Guillemaut, et al., Nucl. Fusion 54 (2014) 093012.
[8] A. Huber, et al., PSI, Nuclear Materials and Energy (2016), doi:10.1016/j.nme.2016.10.027.
[9] S. Wiesen, et al., J. Nucl. Mater. 415 (2011) 535–539.
[10] S.I. Krasheninnikov et al., Phys. Plasmas 4 (5) (May 1997) 1638–1346.
[11] B. Lomanowski, et al., Nucl. Fusion 55 (2015) 123028.
[12] N. Asakura, et al., J. Nucl. Mater. 241 (1997) 559–563.
[13] M.V. Umansky, et al., Phys. Plasmas 5 (1998) 3373.
[14] B. LaBombard, et al., Phys. Plasmas 8 (2001) 2107.
[15] C. Carralero, et al., J. Nucl. Mater. 463 (2015) 123–127.
[16] G.F. Matthews, et al., PSI, Nuclear Materials and Energy (2016), doi:10.1016/j.nme.2016.12.012.
[17] J. Aubert, et al., Fusion Eng. Des. 98–99 (2015) 1206–1210.
[18] R. Wenninger, et al., Nucl. Fusion 55 (2015) 063003.
[19] P.C. Stangeby, The Plasma Boundary of Magnetic Fusion Devices, Taylor and Francis, New York, 2000.
[20] R.A. Pitts, et al., Rev. Sci. Instrum. 74 (2003) 4644.
[21] M. Kocan, et al., PPCF 50 (2008) 125009.
[22] W. Eckstein et al. 2002 Calculated sputtering, reflection and range values IPP Report IPP 9/132 (Garching: Max-Planck-Institut für Plasmaphysik).
[23] S. Brezinsek, et al., J. Nucl. Mater. 463 (2013) S11–S21.
[24] A. Baron-Wiechec, et al., J. Nucl. Mater. 463 (2015) 157–161.
[25] K. Heinola, et al., J. Nucl. Mater. 463 (2015) 961–965.
[26] A. Widdowson, et al., PSI, Nuclear Materials and Energy (2016), doi:10.1016/j.nme.2016.12.008.
[27] N. Catarino, et al., PSI, Nuclear Materials and Energy (2016), doi:10.1016/j.nme.2016.10.027.
[28] S. Brezinsek, et al., Nucl. Fusion 55 (2015) 063021.
[29] S.I. Krasheninnikov, et al., Phys. Plasmas 23 (2016) 055602.